Arsenic-bridged antiferromagnetic superexchange interactions in LaFeAsO

Fengjie Ma,[1,2] Zhong-Yi Lu,[2,*] and Tao Xiang[3,1,†]
[1]*Institute of Theoretical Physics, Chinese Academy of Sciences, Beijing 100190, China*
[2]*Department of Physics, Renmin University of China, Beijing 100872, China*
[3]*Institute of Physics, Chinese Academy of Sciences, Beijing 100190, China*
(Received 27 July 2008; published 18 December 2008; corrected 30 December 2008)

From the first-principles calculations, we have studied the electronic and magnetic structures of LaFeAsO. It is found that a large magnetic moment of $\sim 2.6\mu_B$ is located around each Fe ion, embedded in the environment of itinerant electrons. In the ground state, these local Fe moments are in collinearly antiferromagnetic order, resulting from the interplay between the strong nearest- and next-nearest-neighbor superexchange antiferromagnetic interactions bridged by As atoms. The structure transition observed by the neutron scattering is shown to be magnetically driven. Our study suggests that the antiferromagnetic fluctuation plays an important role in Fe-based superconductors. This sheds light on the understanding of the pairing mechanism in these materials.

DOI: 10.1103/PhysRevB.78.224517 PACS number(s): 74.25.Jb, 71.18.+y, 74.25.Ha, 74.70.−b

I. INTRODUCTION

Recently an iron-based material LaFeAsO was reported to show superconductivity with a transition temperature $T_c \sim 26$ K by partial substitution of O with F atoms.[1] Soon after, other families of Fe-As oxyarsenides with La replaced by Sm,[2] Ce,[3] Pr,[4] and other rare-earth elements were found to be superconducting with T_c of more than 50 K. Like cuprates, these iron arsenides have a layered structure. The superconducting pairing is believed to happen in the iron-based FeAs layers. The high transition temperature and the preliminary band-structure calculation suggest that the superconductivity in these Fe-arsenide superconductors is not mediated by electron-phonon interaction. It is commonly believed that the understanding of electronic structures of the parent compound LaFeAsO is the key to determine the underlying mechanism to make it superconducting upon doping.

The early band-structure calculations suggested that the pure LaFeAsO compound is a nonmagnetic metal, similar to LaFePO,[5] but with strong ferromagnetic or antiferromagnetic instability.[6–8] Later, it was found that the antiferromagnetically ordered state[9,10] has a lower energy than the nonmagnetic one, probably due to the Fermi-surface nesting.[9] However, the band-structure calculations on magnetic properties of LaFeAsO fall into controversy.[11] Dong *et al.*[12] showed that the antiferromagnetic state should form a collinear-striped structure by breaking the rotational symmetry. This collinear-ordered antiferromagnetic state was observed by the neutron-scattering experiments.[13] Furthermore, the neutron-scattering measurement found that there is a structure transition with a monoclinic lattice distortion at ~ 150 K and the collinear order is formed about 15–20 K below this transition temperature. Without this distortion, the square-antiferromagnetic order induced purely by the Fermi-surface nesting is expected to be more stable since there are two orthogonal but equivalent nesting directions (π,π) and $(\pi,-\pi)$, which can lower the energy of the ground state by keeping its rotational symmetry.[9]

The neutron-scattering observation raises the question on the microscopic mechanisms underlying the structural transition and antiferromagnetic transition and the relationship between these two transitions. In this paper, we report the theoretical result on the electronic and magnetic structures of the ground state of LaFeAsO obtained from the thorough first-principles electronic structure calculations; similar calculations were partly reported in Refs. 14 and 15. We find that a large magnetic moment of $\sim 2.6\mu_B$ is formed around each Fe ion and there are strong nearest- and next-nearest-neighbor superexchange antiferromagnetic interactions between these Fe local moments bridged by As atoms. LaFeAsO is metallic since there are itinerant electrons coexisting with Fe local moments. We calculate the nearest- and next-nearest-neighbor superexchange coupling constants and find that they have almost the same amplitude within error of calculation. Their competition affects strongly the electronic structure of LaFeAsO, giving rise to a small monoclinic lattice distortion and a collinear antiferromagnetic ordering of Fe moments, in agreement with the neutron-scattering measurement.

II. COMPUTATIONAL APPROACH

In our calculations the plane-wave basis method was used.[16] We adopted the local (spin) density approximation and the generalized gradient approximation of Perdew *et al.*[17] for the exchange-correlation potentials. The ultrasoft pseudopotentials[18] were used to model the electron-ion interactions. After the full convergence test, the kinetic-energy cutoff and the charge-density cutoff of the plane-wave basis were chosen to be 600 and 4800 eV, respectively. The Gaussian broadening technique was used and a mesh of $16\times16\times8$ k points was sampled for the Brillouin-zone integration. LaFeAsO has a tetragonal layered structure with $P4/nmm$ symmetry. A crystal unit cell consists of eight atoms with alternating FeAs and LaO layers along the c axis. In the calculation, the internal atomic coordinates within the cell were determined by the energy minimization. It was found that the calculated optimized lattice parameters in the antiferromagnetic phase [$a=b=4.035(5)$ Å, $c=8.740$ Å] are

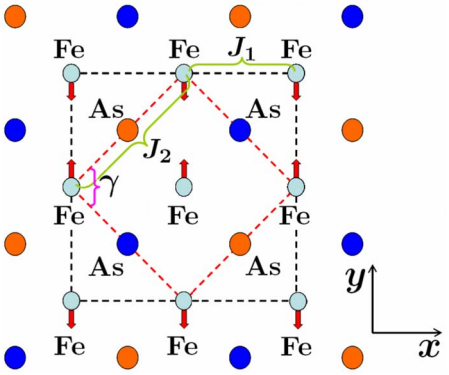

FIG. 1. (Color online) Schematic top view of the FeAs layer in LaFeAsO. The small dashed square is an $a \times a$ unit cell while the large dashed square is a $\sqrt{2}a \times \sqrt{2}a$ unit cell. The collinear-ordered Fe spins in the ground state are shown by arrows.

larger by about 0.8% than the corresponding parameters in the nonmagnetic phase ($a=b=4.004$ Å, $c=8.591$ Å).

III. RESULTS AND ANALYSIS

The previous band-structure calculations[6–10] used an $a \times a \times c$ crystal unit cell as the working cell, in which two Fe, As, La, and O atoms were included. To explore the magnetic structure, in particular the collinear antiferromagnetic state of LaFeAsO, we use a $\sqrt{2}a \times \sqrt{2}a \times c$ unit cell (Fig. 1). In order to determine the values of the nearest- and next-nearest-neighbor coupling constants of spin-spin interaction, J_1 and J_2 (see Fig. 1), we have evaluated the minimal energies of four different magnetic states of Fe ions with imposed constraints if not stable. These four states have nonmagnetic, ferromagnetic, square-antiferromagnetic, and collinear antiferromagnetic orders. If the energy of the nonmagnetic state of LaFeAsO is set to zero, we find that the energies of the ferromagnetic, square-antiferromagnetic, and collinear antiferromagnetic states are 0.0905, −0.010 875, and −0.214 75 eV/Fe, respectively. Thus the ground state is a collinear-ordered antiferromagnetic state, in agreement with the experimental observation.[13]

The magnetic moment around each Fe atom is found to be about $(2.2-2.6)\mu_B$, varying weakly in the above three magnetically ordered states. This suggests that the spin of Fe ions is between 1 and 3/2. The magnetic moment obtained from the neutron-scattering model is about six times smaller than this result. This is probably because the long-range correlated effect, especially the strong competition between different antiferromagnetic states, has not been fully included in the present density-functional theory calculations.

To quantify the antiferromagnetic interactions in this material, we assume that these energy differences are predominantly contributed from the interactions between the Fe spins which can be modeled by the following frustrated Heisenberg model with the nearest- and next-nearest-neighbor couplings J_1 and J_2:

$$H = J_1 \sum_{\langle ij \rangle} \vec{S}_i \cdot \vec{S}_j + J_2 \sum_{\langle\langle ij \rangle\rangle} \vec{S}_i \cdot \vec{S}_j, \tag{1}$$

whereas $\langle ij \rangle$ and $\langle\langle ij \rangle\rangle$ denote the summation over the nearest- and next-nearest neighbors, respectively. From the calculated energy data, we find that $J_1 \sim 0.0498$ eV/S^2 and $J_2 \sim 0.0510$ eV/S^2. If the spin of each Fe ion $S=1$, then $J_1 \sim 0.0498$ eV and $J_2 \sim 0.0510$ eV. (The detailed calculation is given in the Appendix.)

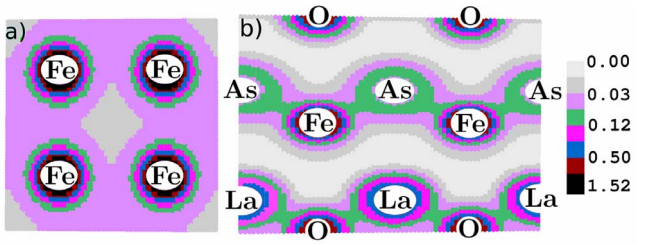

FIG. 2. (Color online) Charge-density distribution (e/bohr^3) of LaFeAsO (a) in the (001) plane crossing Fe-Fe atoms and (b) in the (110) plane crossing Fe-As-Fe atoms.

The above result indicates that there are competing antiferromagnetic interactions between the Fe spins. In particular, the antiferromagnetic coupling between two next-nearest-neighboring Fe spins is very strong. This will frustrate the spin Néel structure and give rise to a collinear-ordered antiferromagnetic ground state.

To explore the origin of these antiferromagnetic interactions, we have calculated the charge distribution around Fe and As ions. The result [see Figs. 2(a) and 2(b)] shows that there is almost no charge distribution between two diagonal Fe atoms but there is a strong bonding between Fe and As ions. This indicates that the antiferromagnetic coupling J_2 is induced by the superexchange bridged by As ions. This superexchange is antiferromagnetic because the intermediated state associated with the hopping bridged by As ions is a spin singlet.

The charge distribution between two nearest Fe ions is finite. Thus there is a direct exchange interaction between two neighboring Fe spins. Since there is a strong Hund's coupling between the spins of $3d$ electrons within each Fe ion, the direct exchange interaction is found to be ferromagnetic when the distance of two Fe atoms is between 2.4 and 2.85 Å. However, the overall magnetic coupling J_1 between the two nearest Fe spins in LaFeAsO is antiferromagnetic. Thus J_1 is also dominated by the superexchange interaction bridged by As $4p$ orbitals.

In the collinear antiferromagnetic phase, we find that a small structural relaxation, for which the lattice is slightly expanded along the spin-antiparallel ordering direction (y axis in Fig. 1) and slightly shrunk along the spin-parallel ordering direction (x axis in Fig. 1), can further lower the ground-state energy. This changes the angle between two principal axes in the ab plane, γ, from 90° to 90.47°. The corresponding energy gain is 7 meV. However, we find that this small lattice distortion affects weakly the band structure and the Fe moments.

Here we emphasize that our calculations show that the driving force upon this structural distortion is nothing but the magnetic interaction. More specifically, it is the superexchange interaction J_2 that breaks the rotational symmetry leading to both the structural distortion and the Fe-spin collinearly antiferromagnetic ordering. In reality the structure transition will take place when the antiferromagnetic spin-

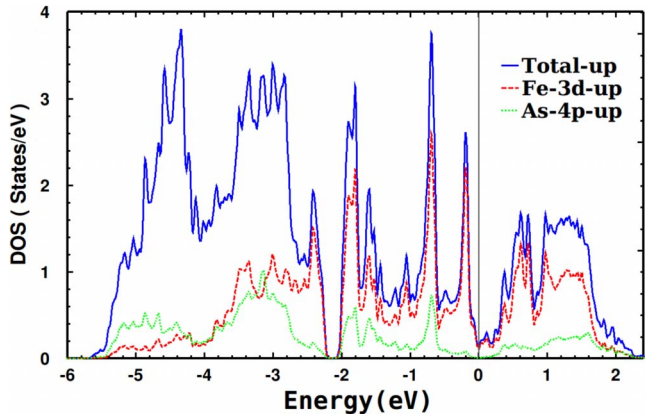

FIG. 3. (Color online) Total and orbital-resolved partial densities of states per f.u. (spin-up part) of LaFeAsO in the collinear antiferromagnetic state. The Fermi energy is set to zero.

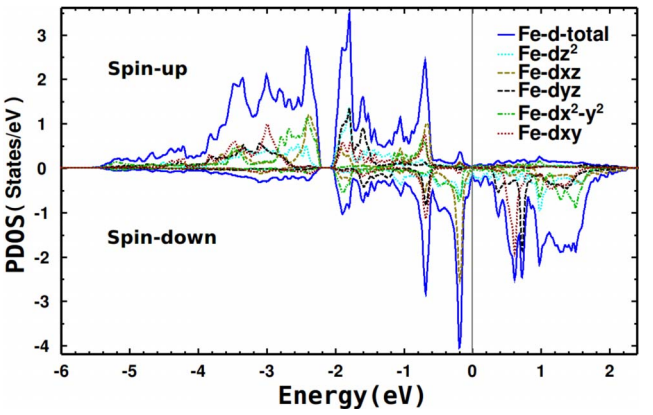

FIG. 4. (Color online) Total and projected densities of states at the five Fe 3*d* orbitals around one Fe atom. The Fermi energy is set to zero.

fluctuation energy is higher than the thermal fluctuation energy, while the collinear antiferromagnetic phase transition will then take place when the spin-correlation energy further surpasses the quantum fluctuation energy. This explains why the monoclinic lattice distortion happens at about 150 K prior to the Fe-spin collinearly antiferromagnetic order appearing at about 134 K.[13]

In our calculations the parallel and antiparallel alignments of the Fe spins between two neighboring FeAs layers bridged by oxygen atoms are essentially degenerate. Thus the neutron-observed antiparallel alignment between the neighboring FeAs layers[13] is likely to be due to the entropy.

Figure 3 shows the total and projected densities of states of LaFeAsO in the collinear antiferromagnetic phase. In comparison with the nonmagnetic phase, we find that most of the states around the Fermi level are gapped by the collinear antiferromagnetic order. This suppresses the total carrier density by more than 2 orders of magnitude. The strong suppression is consistent with the Hall-coefficient measurement which shows that the absolute value of the Hall coefficient is enhanced by more than 150 times in the antiferromagnetic phase at 4 K versus the nonmagnetic phase above 150 K. Furthermore, we find that the density of states at the Fermi level is also suppressed in comparison with the nonmagnetic state.[9] However, it is not suppressed as strongly as the total carrier density. The corresponding electronic specific-heat coefficients are 0.65 (collinear antiferromagnetic state) and 4.28 $\mathrm{mJ/(K^2\ mol)}$ (nonmagnetic state). This is also consistent with the specific-heat measurement.

We have also calculated the band structure of LaFeAsO with 5% F doping or 5% Sr doping by taking the virtual-crystal approximation in the collinear antiferromagnetic phase. We find that the overall band structure is hardly changed by 5% electron or hole doping. The Fe moment is also unchanged. Only the Fermi energy moves up or down with electron or hole doping. However, as shown in Fig. 5 the Fermi surface changes dramatically.

By projecting the density of states onto the five 3*d* orbitals of Fe (Fig. 4), we find that the five up-spin orbitals are almost completely filled and the five down-spin orbitals are only partially filled. However, the down-spin electrons are nearly uniformly distributed in these five 3*d* orbitals. This indicates that the crystal-field splitting imposed by As atoms is relatively small and the Fe 3*d* orbitals hybridize strongly with each other. As Hund's rule coupling is strong, this would lead to a large magnetic moment formed around each Fe atom, as found in our calculations. The frustration between the J_1 and J_2 terms will suppress strongly the antiferromagnetic ordering at the two Fe sublattices, each connected only by the J_2 terms. This, together with the quantum fluctuation, will reduce strongly the average magnetic moment around each Fe measured by experiments.

Figure 5 shows the electronic band structure and the Fermi surfaces in the collinear antiferromagnetic state. Unlike in the nonmagnetic state, there are now only three Fermi-surface sheets in the undoped case, one small hole cylinder along ΓZ and two small electron pockets formed between Γ and $\bar{X}$, crossing the Fermi level. From the volumes enclosed by these Fermi surfaces, we find that the hole carrier density is about $1.64\times10^{19}/\mathrm{cm}^3$ and the electron carrier density is about $0.94\times10^{19}/\mathrm{cm}^3$. Both decrease by more than 2 orders of magnitude in comparison to the nonmagnetic or square-antiferromagnetic states.[9] Upon F (Sr) doping, the electron (hole) Fermi-surface sheets expand while the hole (electron) Fermi-surface sheets shrink. With 5% F (Sr) doping, the whole Fermi surface becomes electron (hole)-like and the corresponding electron (hole) carrier density is $6.31\times10^{20}/\mathrm{cm}^3$ $(7.01\times10^{20}/\mathrm{cm}^3)$, increasing by about 25 times compared with total carrier density in the undoped case.

IV. DISCUSSION IN CONNECTION WITH SUPERCONDUCTIVITY

The above discussion shows that there are strong nearest- and next-nearest-neighbor superexchange interactions in LaFeAsO. The interplay between these antiferromagnetic interactions can affect strongly the magnetic structure of the ground state. Upon doping, the antiferromagnetic ordering will be suppressed. However, we believe that the remanent antiferromagnetic fluctuation will survive, similar to cuprate superconductors. Thus the effective low-energy model for

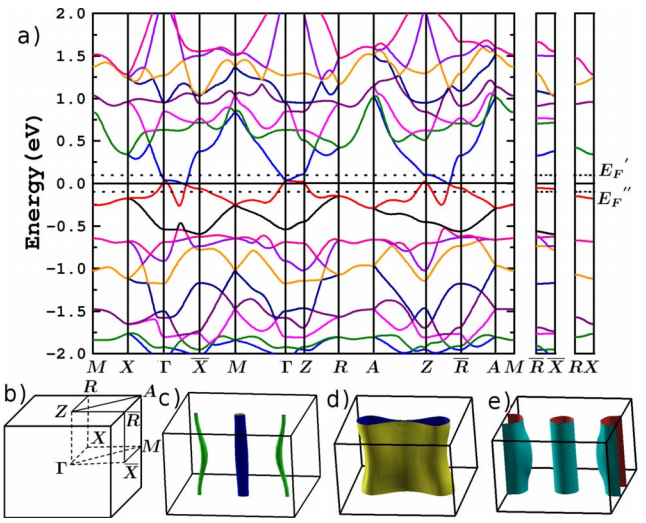

FIG. 5. (Color online) (a) The electronic band structure of LaFeAsO in the collinear-ordered antiferromagnetic state with the in-plane angle $\gamma=90.47°$ (see Fig. 1 for the definition of γ). The Fermi energy is set to zero. E_F' and E_F'' correspond to 5% F-doping and 5% Sr-doping cases, respectively. (b) The Brillouin zone. (c) The Fermi surface of the undoped compound, one holelike cylinder along ΓZ and two electronlike pockets between Γ and $\bar{X}$. ΓX corresponds to the parallel-aligned moment line and $\Gamma\bar{X}$ corresponds to the antiparallel-aligned moment line. (d) The Fermi surface of the 5% F-doped compound. (e) The Fermi surface of the 5% Sr-doped compound.

describing these Fe-based superconductors, whether it is a single-band or multiband Hamiltonian, should include the frustrated Heisenberg terms defined by Eq. (1).

In the Fe-based superconductors, the magnetic fluctuation, induced by either the antiferromagnetic superexchange interactions or the on-site Hund's rule coupling, can be responsible for the superconducting pairing. The former interaction favors a spin singlet pairing, while the latter favors a spin triplet pairing. However, the superconductivity induced by Hund's rule coupling would generally involve the interband pairing, which is limited by the available phase space if the total momentum of Cooper pair is zero. This would suggest that the spin triplet pairing is not energetically favorable in a system with strong antiferromagnetic fluctuations. Moreover, from the study of high-T_c cuprate superconductivity, we know that the strong next-nearest-neighbor antiferromagnetic interaction favors an extended s-wave or d_{xy}-wave pairing. Therefore, we believe that the leading pairing instability will be in spin singlet channel if the superconductivity is driven by the antiferromagnetic fluctuation. However, the competing nearest-neighbor antiferromagnetic interaction may introduce a small other component with different symmetries, for example, a $d_{x^2-y^2}$-wave gap, to the pairing function. Thus the resulting gap parameter will generally be a superposition of two components with different symmetries, for example, an extended s plus $d_{x^2-y^2}$ pairing state.

The above analysis suggests that there are some similarities between pnictide and cuprate superconductors. Here we would also like to further address that the difference between them is that the undoped cuprate is an antiferromagnetic Mott insulator while the undoped LaFeAsO is an antiferromagnetic semimetal. In particular, in undoped LaFeAsO there already coexist both local magnetic moments and itinerant electrons. This is similar as in the doped cuprate superconductors. In cuprate superconductors, the low-energy physics can be effectively described by the t-J model, in which the coupling between local spins is the antiferromagnetic interaction and the doped holes or electrons can hop on the lattice. Similarly, one would expect that the low-energy physics of doped LaFeAsO can be effectively described by a multiband model with strong antiferromagnetic interactions.

V. CONCLUSION

In conclusion, we have presented the first-principles calculations of the electronic structure of LaFeAsO. We find that there are strong antiferromagnetic nearest- and next-nearest-neighbor superexchange interactions between Fe local moments bridged by As $4p$ orbitals. The next-nearest-neighbor antiferromagnetic coupling is comparable to the nearest-neighbor one. This gives rise to the collinear antiferromagnetic ordering of Fe spins in the ground state, in agreement with the measurement data of neutron scattering. The existence of strong antiferromagnetic fluctuations in Fe-based superconductors bears a strong analogy to high-T_c cuprates. This suggests that the superconductivity in these two different kinds of high-T_c materials may have a common origin.

Note added. Recently, we learned of the works of Si and Abrahams[19] and of Ishibashi *et al.*[20] In the former, it is conjectured that there is antiferromagnetic interaction between the next-nearest-neighbor Fe-Fe atoms but ferromagnetic interaction between the nearest-neighbor Fe-Fe atoms. The latter reports the similar band structures on LaFeAsO but does not explore the mechanism underlying the magnetic structures and properties.

ACKNOWLEDGMENTS

We wish to thank N. L. Wang, J. L. Luo, P. Dai, Y. H. Su, and H. G. Luo for fruitful discussions. This work was partially supported by the National Natural Science Foundation of China and by the National Program for Basic Research of MOST, China.

APPENDIX: DETERMINATION OF J_1 AND J_2 IN FRUSTRATED HEISENBERG MODEL

To determine the value of J_1, one needs to first evaluate the energy of a pair of the nearest Fe-Fe moments in parallel ($E_{F,1}$) and antiparallel ($E_{A,1}$) alignments with respect to a nonmagnetic reference state. Then from their difference, one can determine the value of J_1 by the following formula:

$$J_1 = (E_{F,1} - E_{A,1})/(2S^2), \tag{A1}$$

where S is the spin of each Fe ion. It should be emphasized that $E_{F,1}$ is not necessary to be equal to $-E_{A,1}$ since the energy of the reference state may not be located exactly at the middle of the energy between the ferromagnetic and an-

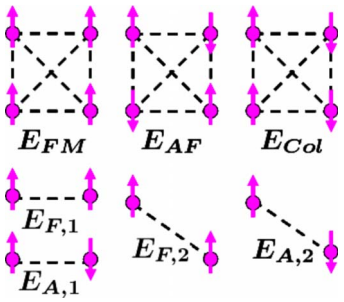

FIG. 6. (Color online) The three magnetic configurations, namely, ferromagnetic (E_{FM}), square-antiferromagnetic (E_{AF}), and collinear antiferromagnetic (E_{col}) configurations and the magnetic bond energies $E_{F,1}$ and $E_{A,1}$ between the nearest Fe-Fe moments and $E_{F,2}$ and $E_{A,2}$ between the next-nearest Fe-Fe moments.

tiferromagnetic states. This energy lineup between the nonmagnetic and any other magnetic state needs self-consistent total-energy calculations to determine that is what we have done. Thus $E_{F,1}$ and $E_{A,1}$ should be determined independently. Similarly, J_2 can be determined from the difference between the energy of a pair of next-nearest Fe-Fe moments in the parallel ($E_{F,2}$) and antiparallel ($E_{A,2}$) alignments,

$$J_2 = (E_{F,2} - E_{A,2})/(2S^2). \tag{A2}$$

To determine the values of $E_{F,1}-E_{A,1}$ and $E_{F,2}-E_{A,2}$, we have calculated the total energies of the ferromagnetic (E_{FM}), square-antiferromagnetic (E_{AF}), and collinear antiferromagnetic (E_{col}) states. The spin configurations of these three states are shown in Fig. 6. The corresponding energy differences with respect to the nonmagnetic state (E_{NM}) are 0.0905, −0.108 75, and −0.214 75 eV/Fe. If these energy differences result mainly from the exchange interactions between the nearest- and next-nearest Fe moments, then we obtain the following equations:

$$E_{\mathrm{FM}} - E_{\mathrm{NM}} = 2E_{F,1} + 2E_{F,2} = 0.0905 \text{ eV},$$

$$E_{\mathrm{AF}} - E_{\mathrm{NM}} = 2E_{A,1} + 2E_{F,2} = -0.108\ 75 \text{ eV},$$

$$E_{\mathrm{col}} - E_{\mathrm{NM}} = E_{F,1} + E_{A,1} + 2E_{A,2} = -0.214\ 75 \text{ eV}.$$

From them, we further find that

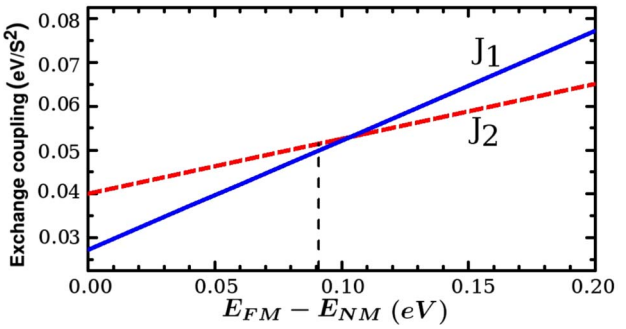

FIG. 7. (Color online) Variations in J_1 and J_2 with $E_{\mathrm{FM}}-E_{\mathrm{NM}}$. The dashed line denotes our calculated value.

$$E_{F,1} - E_{A,1} = 0.0996 \text{ eV},$$

$$E_{F,2} - E_{A,2} = 0.1028 \text{ eV}.$$

Thus the values of J_1 and J_2 are

$$J_1 = 0.0498 \text{ eV/S}^2, \tag{A3}$$

$$J_2 = 0.0501 \text{ eV/S}^2. \tag{A4}$$

The energy of the current ferromagnetic state is less accurately determined since this state is not a stable state. The error in $E_{\mathrm{FM}}-E_{\mathrm{NM}}$ will give rise to the error in J_1 and J_2. Figure 7 shows how J_1 and J_2 change with $E_{\mathrm{FM}}-E_{\mathrm{NM}}$. As we see, we find that $J_2 > J_1/2$ even when we assume that the deviation of $E_{\mathrm{FM}}-E_{\mathrm{NM}}$ from our calculated value is as big as 0.1 eV. Thus we believe that the collinear antiferromagnetic order observed in LaFeAsO is indeed due to the competition of superexchange interactions.

The above estimation indicates that J_1 is close to J_2 within the error of calculation for LaFeAsO. In this parameter range, as shown in Ref. 21 with the spin-wave approximation, the J_1 superexchange interaction term will compete strongly with the J_2 term. This results in a strong reduction in the magnetic moment of Fe, which would naturally explain why the observed magnetic moment ($\sim 0.36\mu_B$) is significantly smaller than that obtained from the density-functional calculations for LaFeAsO.

*zlu@ruc.edu.cn
†txiang@aphy.iphy.ac.cn

[1] Y. Kamihara, T. Watanabe, M. Hirano, and H. Hosono, J. Am. Chem. Soc. **130**, 3296 (2008).
[2] X. H. Chen, T. Wu, G. Wu, R. H. Liu, H. Chen, and D. F. Fang, Nature (London) **453**, 761 (2008).
[3] G. F. Chen, Z. Li, D. Wu, G. Li, W. Z. Hu, J. Dong, P. Zheng, J. L. Luo, and N. L. Wang, Phys. Rev. Lett. **100**, 247002 (2008).
[4] Z. A. Ren, J. Yang, W. Lu, W. Yi, G. C. Che, X. L. Dong, L. L. Sun, and Z. X. Zhao, Mater. Res. Innovations **12**, 105 (2008).
[5] S. Lebegue, Phys. Rev. B **75**, 035110 (2007).
[6] D. J. Singh and M. H. Du, Phys. Rev. Lett. **100**, 237003 (2008).
[7] G. Xu, W. Ming, Y. Yao, X. Dai, S. C. Zhang, and Z. Fang, Europhys. Lett. **82**, 67002 (2008).
[8] K. Haule, J. H. Shim, and G. Kotliar, Phys. Rev. Lett. **100**, 226402 (2008).
[9] F. Ma and Z.-Y. Lu, Phys. Rev. B **78**, 033111 (2008).
[10] C. Cao, P. J. Hirschfeld, and H. P. Cheng, Phys. Rev. B **77**, 220506(R) (2008).
[11] I. I. Mazin, M. D. Johannes, L. Boeri, K. Koepernik, and D. J. Singh, Phys. Rev. B **78**, 085104 (2008).
[12] J. Dong, H. J. Zhang, G. Xu, Z. Li, G. Li, W. Z. Hu, D. Wu, G. F. Chen, X. Dai, J. L. Luo, Z. Fang, and N. L. Wang, Europhys. Lett. **83**, 27006 (2008).

[13] C. de la Cruz, Q. Huang, J. W. Lynn, J. Li, W. Ratcliff II, J. L. Zarestky, H. A. Mook, G. F. Chen, J. L. Luo, N. L. Wang, and P. Dai, Nature (London) **453**, 899 (2008).
[14] T. Yildirim, Phys. Rev. Lett. **101**, 057010 (2008).
[15] Z. P. Yin, S. Lebegue, M. J. Han, B. P. Neal, S. Y. Savrasov, and W. E. Pickett, Phys. Rev. Lett. **101**, 047001 (2008).
[16] S. Baroni, A. Dal Corso, S. de Gironcoli, P. Giannozzi, C. Cavazzoni, G. Ballabio, S. Scandolo, G. Chiarotti, P. Focher, A. Pasquarello, K. Laasonen, A. Trave, R. Car, N. Marzari, and A. Kokalj, http://www.quantum-espresso.org
[17] J. P. Perdew, K. Burke, and M. Ernzerhof, Phys. Rev. Lett. **77**, 3865 (1996).
[18] D. Vanderbilt, Phys. Rev. B **41**, 7892 (1990).
[19] Q. Si and E. Abrahams, Phys. Rev. Lett. **101**, 076401 (2008).
[20] S. Ishibashi, K. Terakura, and H. Hosono, arXiv:0804.2963, J. Phys. Soc. Jpn. (to be published).
[21] D. X. Yao and E. W. Carlson, Phys. Rev. B **78**, 052507 (2008).